



Contents lists available at ScienceDirect

Journal of Quantitative Spectroscopy & Radiative Transfer

journal homepage: www.elsevier.com/locate/jqsrt

Separation of variables method for multilayered nonspherical particles

Alexander Vinokurov^{a,*}, Victor Farafonov^a, Vladimir Il'in^{b,c}^a St. Petersburg University of Aerospace Instrumentation, Bol. Morskaya 67, St. Petersburg 190000, Russia^b Astronomical Institute, St. Petersburg State University, Universitetskij pr. 28, St. Petersburg 198504, Russia^c Pulkovo Astronomical Observatory, Pulkovskoe shosse 65/1, St. Petersburg 196140, Russia

ARTICLE INFO

Article history:

Received 29 December 2008

Received in revised form

27 February 2009

Accepted 27 February 2009

PACS:

42.25Fx

Keywords:

Light scattering

Separation of variables' method

Nonspherical inhomogeneous scatterers

ABSTRACT

A separation of variables method based on expansions of the electromagnetic fields in terms of spherical wave functions is expanded at nonspherical (axisymmetric) particles with a rather large number of layers. Commonly used alternative approaches to systems of linear algebraic equations relative to unknown field expansion coefficients for layered particles are considered in some detail. The SVM code developed is compared with the EBCM, GMT and DDA codes designed for multilayered scatterers and some numerical results obtained for nonspherical scatterers with up to 100 layers are presented as illustrations.

© 2009 Elsevier Ltd. All rights reserved.

1. Introduction

Light scattering by layered particles is of growing interest for modelling optical properties of disperse media studied in astrophysics, physics of atmosphere and oceans, ecology, biophysics as well as in various applications. Such particles are applied to represent natural scatterers of both quasilayered and more complex structures. A large number of methods have been used to treat layered particles, but this field has been never reviewed in sufficient detail. Therefore, a state of the art review is required.

The *separation of variables method* (SVM) was most often applied to treat light scattering by layered scatterers (see [1,2]). There are numerous works devoted to layered *spheres* as the SVM solution (theory) of Mie [3] is easily extended to such spheres (see for details [4]). After the first paper of Aden and Kerker [5] on core-mantle spheres, there were dozens papers where this theory was refined and applied to different cases (see reviews in [6,7]). New works on the subject appear till now (see, e.g., [8–11]).

The SVM using a cylindrical basis was utilized to obtain solutions for layered infinite *cylinders* which find some useful applications. Pioneer works were made on core-mantle circular cylinders by Kerker and Matijevich [12] and Shah [13]. Recent studies are presented in [14–16].

The SVM with a spheroidal basis was applied first to core-mantle *spheroids* [17] and later to multilayered ones (see a review [18] and recent papers [19–23]). Note that in all the works the particles had spheroidal layers with *confocal*

* Corresponding author. Tel.: +7 812 7832236; fax: +7 812 4287129.

E-mail address: alexander.a.vinokurov@gmail.com (A. Vinokurov).

boundaries. A breakthrough was made by Han et al. [24] who obtained an exact solution for spheroids with nonconfocal layers.

Layered scatterers of arbitrary (but usually axisymmetric) shape were treated by the *extended boundary condition method* (EBCM) using a spherical basis and the *T-matrix method* (TMM). The classic works are a theoretical paper of Peterson and Ström [25] and a work of Wang and Barber [26] with numerical results. Many papers that apply this approach to layered scatterers are cited in comprehensive reviews of Mishchenko et al. [27–29]. We note two interesting modifications of the approach. Kyurkchan et al. [31] have extended their modification of the EBCM called pattern equation method to coated scatterers. The approach deals with scattering patterns representing the fields in the far field zone and is easily generalized on multilayered objects. Petrov et al. [30] have calculated the *T-matrix* for a scatterer with layered structure from a *Sh-matrix* that depends only on the shape of the layers (no dependence on their size parameters and refractive indices). The authors expand their approach at continuously varying layer parameters.

Two methods mainly distinguished by use of different basis—the (generalized) *point-matching method* (PMM) and the *generalized multipole technique* (GMT) are close to the EBCM/TMM approach. Al-Rizzo and Tranquilla [32] have demonstrated that the generalized PMM can be efficiently applied to core-mantle axisymmetric scatterers. Doicu and Wriedt [33,34] have combined their null-field method with discrete sources (actually the GMT) with the TMM to treat layered three-dimensional scatterers of rather large eccentricity.

Other methods—the coupled dipole method (CDM), the method of moments (MoM), the finite difference time domain method (FDTD), etc. [1,2] are more universal and hence much more computational time consuming than the SVM, EBCM, PMM and GMT when applied to simple shape scatterers. Therefore, the CDM, MoM, FDTD, etc. are mainly used for complicated objects.

The discrete dipole approximation (DDA) is a typical representative of the CDM methods based on the volume integral formulation of the scattering problem. Core-mantle ellipsoids are involved in the standard DDA code of Draine and Flatau [35]. An example of application of the DDA to complex core-mantle particles can be found in [36].

The FDTD method was applied to quite different layered objects: antennas [37], biological tissues [39], human head [38], etc. This method is often used also to consider optical properties of layered media (see, e.g., [41]). Some other methods recently modified to treat layered particles are presented in [42–44] (see, e.g., [45] for references to earlier works).

Besides the methods mentioned, some *approximations* can be also useful in study of layered scatterers. Multilayered ellipsoids in the Rayleigh (RA) and quasistatic (QSA) approximations were considered, for instance, in [46]. Layered spheres have been recently studied in the Rayleigh–Gans approximation in [47]. The anomalous diffraction (van de Hulst's) and geometrical optics approximations are applied to multilayered particles in [48]. Another way to approximate the optical properties of layered scatterers is the effective medium theory (EMT—see for more details [49]). A special rule of this theory for layered particles was described in [50]. The EMT is very efficient, but may be inaccurate in particular for layered scatterers (see discussion in [51]). Naturally, any of the approximations has an essentially limited accuracy level and applicability range.

Three notes should be added. First, particles with an (large) inclusion can be considered as core-mantle ones. However, we skipped references to most papers on such particles as the main attention is paid here to multilayered scatterers. Second, it should be mentioned that there are many not works on scattering of acoustic waves by layered obstacles (e.g., [52,53]). Third, because of application demands essential efforts were directed at solution of the inverse problem for layered scatterers and some interesting results have been obtained (see, e.g., [54,55]).

Numerous works recently done on wave scattering by layered particles reflects the fact that they provide a very useful model for various inhomogeneous natural scatterers. Though many methods were applied or specially developed to treat nonspherical particles with layers, it is still hardly possible to derive sufficiently accurate results when the number of (nonspheroidal) layers exceeds 5–10.

In this paper, the SVM based on expansions of the fields in terms of spherical wave functions is applied to really multilayered nonspherical (axisymmetric) particles. In Section 2 main features of our approach (separation of the fields, special scalar potentials used, etc.) are described. Two alternatives used to solve systems of linear algebraic equations relative to the scattered field expansion coefficients are discussed in some detail. In Section 3 we consider convergence, accuracy and speed of our SVM approach. It is compared with the EBCM, GMT, DDA methods applied to multilayered scatterers. Some numerical results for multilayered scatterers are also presented. Main conclusions are drawn in Section 4.

2. Basic equations

2.1. Formulation of the problem

We consider an \mathcal{L} -layered scatterer embedded in a homogeneous medium. All layer boundaries S_i ($i = 1, 2, \dots, \mathcal{L}$) are assumed to be axisymmetric and to have the same symmetry axis. The boundaries divide the particle and the medium into domains D_i ($i = 1, 2, \dots, \mathcal{L} + 1$). They are characterized by dielectric permittivity ε_i and magnetic permeability μ_i (see Fig. 1), the corresponding wave number is $k_i = \sqrt{\varepsilon_i \mu_i} k_0$, where k_0 is the wave number in vacuum.

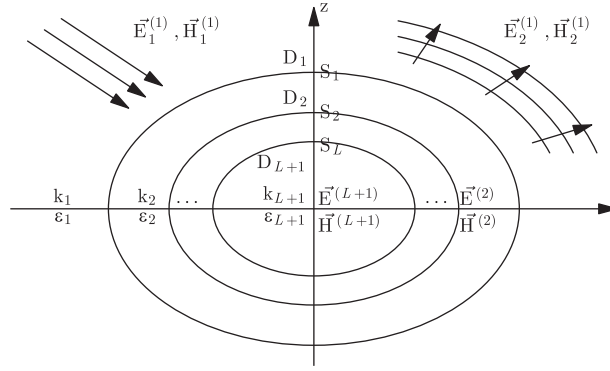


Fig. 1. An axisymmetric layered scatterer (z -axis coincides with the symmetry one) and notation used.

The electromagnetic fields in the domain D_i are denoted by $\mathbf{E}^{(i)}, \mathbf{H}^{(i)}$. The fields satisfy the Maxwell equations

$$\begin{cases} \mathbf{E}^{(i)}(\mathbf{r}) = -\frac{1}{i\epsilon_i k_0} \nabla \times \mathbf{H}^{(i)}(\mathbf{r}), & \mathbf{r} \in D_i, \\ \mathbf{H}^{(i)}(\mathbf{r}) = \frac{1}{i\mu_i k_0} \nabla \times \mathbf{E}^{(i)}(\mathbf{r}), & \mathbf{r} \in D_i, \end{cases} \quad (1)$$

where $i = 1, 2, \dots, \mathcal{L} + 1$. The boundary conditions at all the layer surfaces are

$$\begin{cases} \mathbf{E}^{(i)}(\mathbf{r}) \times \mathbf{n}_i(\mathbf{r}) = \mathbf{E}^{(i+1)}(\mathbf{r}) \times \mathbf{n}_i(\mathbf{r})|_{\mathbf{r} \in S_i}, \\ \mathbf{H}^{(i)}(\mathbf{r}) \times \mathbf{n}_i(\mathbf{r}) = \mathbf{H}^{(i+1)}(\mathbf{r}) \times \mathbf{n}_i(\mathbf{r})|_{\mathbf{r} \in S_i}, \end{cases} \quad (2)$$

where $\mathbf{n}_i(\mathbf{r})$ is the outer normal to the surface S_i and $i = 1, 2, \dots, \mathcal{L}$.

The fields $\mathbf{E}^{(i)}, \mathbf{H}^{(i)}$ in the domains D_i with $i \leq \mathcal{L}$ should be represented by sums of incoming and outgoing fields

$$\mathbf{E}^{(i)} = \mathbf{E}_1^{(i)} + \mathbf{E}_2^{(i)}, \quad \mathbf{H}^{(i)} = \mathbf{H}_1^{(i)} + \mathbf{H}_2^{(i)}. \quad (3)$$

In the innermost layer (a particle core) like inside a homogeneous particle one has just $\mathbf{E}^{(\mathcal{L}+1)} = \mathbf{E}_1^{(\mathcal{L}+1)}, \mathbf{H}^{(\mathcal{L}+1)} = \mathbf{H}_1^{(\mathcal{L}+1)}$. As the scattered field must satisfy the Sommerfeld radiation condition at infinity and an incident plane wave can be represented by incoming waves, we can denote the former by $\mathbf{E}_2^{(1)}, \mathbf{H}_2^{(1)}$ and the latter by $\mathbf{E}_1^{(1)}, \mathbf{H}_1^{(1)}$ when considering the fields outside the particle.

Thus, the problem is to find the unknown scattered field $(\mathbf{E}_2^{(1)}, \mathbf{H}_2^{(1)})$ as a solution to Eqs. (1) with the boundary conditions (2) for the given incident plane wave $(\mathbf{E}_1^{(1)}, \mathbf{H}_1^{(1)})$.

2.2. Features of the approach used

To solve the problem we apply the SVM with a spherical basis. The following generalization of this method on nonspherical scatterers is used. All the fields are expanded in terms of spherical wave functions, the expansions are substituted in boundary conditions, and then integration of these conditions over the boundaries gives a system of linear equations relative to unknown scattered field expansion coefficients (see for more details, e.g., [56,57]).

We extend this approach to layered scatterers and modify it by extracting an axisymmetric part of the fields and utilizing special scalar potentials for different parts of the fields.

For each domain D_i , the fields $\mathbf{E}_s^{(i)}, \mathbf{H}_s^{(i)}$ ($s = 1, 2; i = 1, 2, \dots, \mathcal{L} + 1$) are divided in two parts:

$$\mathbf{E}_s^{(i)} = \mathbf{E}_{s,A}^{(i)} + \mathbf{E}_{s,N}^{(i)}, \quad \mathbf{H}_s^{(i)} = \mathbf{H}_{s,A}^{(i)} + \mathbf{H}_{s,N}^{(i)}, \quad (4)$$

where the fields $\mathbf{E}_{s,A}^{(i)}, \mathbf{H}_{s,A}^{(i)}$ do not depend on the azimuthal angle φ and are hereafter called *axisymmetric*. Averaging of the *nonaxisymmetric* parts $\mathbf{E}_{s,N}^{(i)}, \mathbf{H}_{s,N}^{(i)}$ over this angle should give zero. It is simple to prove that the light scattering problem can be solved independently for axisymmetric ($\mathbf{E}_A = \mathbf{E}_{1,A} + \mathbf{E}_{2,A}$) and nonaxisymmetric ($\mathbf{E}_N = \mathbf{E}_{1,N} + \mathbf{E}_{2,N}$) parts of the fields [58]. Such representation of the fields has advantages and disadvantages discussed in [59] and can be easily skipped.

Special scalar potentials are introduced for each of the field parts. For the axisymmetric parts, we employ

$$p_s^{(i)} = E_{s,A,\varphi}^{(i)} \cos \varphi, \quad q_s^{(i)} = H_{s,A,\varphi}^{(i)} \cos \varphi, \quad (5)$$

where $E_{s,A,\varphi}^{(i)}, H_{s,A,\varphi}^{(i)}$ are φ -components of the fields $\mathbf{E}_{s,A}^{(i)}$ and $\mathbf{H}_{s,A}^{(i)}$. Other components of the fields are derived from the Maxwell equations. The potentials $p^{(i)}, q^{(i)}$ resemble the Abraham ones, but in contrast to them satisfy the corresponding Helmholtz equations [60]. It is possible to show that the boundary conditions for $p^{(i)}$ and $q^{(i)}$ can be separated, with p being related to the TE mode task and q to the TM mode one (see for more details [59]). A definition of the TE and TM modes is

given, e.g., in [49]. Spherical coordinates (r, θ, φ) related with the axisymmetric particle are introduced in such a way that all layer surface equations take the form $r = r_i(\theta)$.

In the case of the nonaxisymmetric parts, for the TE mode we use

$$\mathbf{E}_{s,N}^{(i)} = \nabla \times (U_s^{(i)} \mathbf{i}_z + V_s^{(i)} \mathbf{r}), \quad \mathbf{H}_{s,N}^{(i)} = \frac{1}{i\mu_i k_0} \nabla \times \nabla \times (U_s^{(i)} \mathbf{i}_z + V_s^{(i)} \mathbf{r}), \quad (6)$$

and for the TM mode

$$\mathbf{E}_{s,N}^{(i)} = \frac{1}{i\epsilon_i k_0} \nabla \times \nabla \times (U_s^{(i)} \mathbf{i}_z + V_s^{(i)} \mathbf{r}), \quad \mathbf{H}_{s,N}^{(i)} = \nabla \times (U_s^{(i)} \mathbf{i}_z + V_s^{(i)} \mathbf{r}), \quad (7)$$

where \mathbf{i}_z is the unit vector along the particle symmetry axis.

As the scalar potentials introduced satisfy Helmholtz equations they can be expanded in terms of spherical functions as follows:

$$\begin{aligned} p_1^{(i)} &= \sum_{l=1}^{\infty} a_{1,l}^{(i)} j_l(k_i r) P_l^1(\cos \theta) \cos \varphi, & U_1^{(i)} &= \sum_{m=1}^{\infty} \sum_{l=m}^{\infty} a_{1,lm}^{(i)} j_l(k_i r) P_l^m(\cos \theta) \cos m\varphi, \\ q_1^{(i)} &= \sum_{l=1}^{\infty} b_{1,l}^{(i)} j_l(k_i r) P_l^1(\cos \theta) \sin \varphi, & V_1^{(i)} &= \sum_{m=1}^{\infty} \sum_{l=m}^{\infty} b_{1,lm}^{(i)} j_l(k_i r) P_l^m(\cos \theta) \sin m\varphi, \end{aligned} \quad (8)$$

$$\begin{aligned} p_2^{(i)} &= \sum_{l=1}^{\infty} a_{2,l}^{(i)} h_l^{(1)}(k_i r) P_l^1(\cos \theta) \cos \varphi, & U_2^{(i)} &= \sum_{m=1}^{\infty} \sum_{l=m}^{\infty} a_{2,lm}^{(i)} h_l^{(1)}(k_i r) P_l^m(\cos \theta) \cos m\varphi, \\ q_2^{(i)} &= \sum_{l=1}^{\infty} b_{2,l}^{(i)} h_l^{(1)}(k_i r) P_l^1(\cos \theta) \sin \varphi, & V_2^{(i)} &= \sum_{m=1}^{\infty} \sum_{l=m}^{\infty} b_{2,lm}^{(i)} h_l^{(1)}(k_i r) P_l^m(\cos \theta) \sin m\varphi, \end{aligned} \quad (9)$$

where $h_l^{(1)}(k_i r)$ and $j_l(k_i r)$ are the first kind Hankel and Bessel functions, $P_l^m(\cos \theta)$ the associated Legendre functions. So, to find the scattered field at any point \mathbf{r} we need to determine the expansion coefficients $a_{2,l}^{(1)}$, $b_{2,l}^{(1)}$ and $a_{2,lm}^{(1)}$, $b_{2,lm}^{(1)}$. Naturally, the optical properties of a scatterer such as cross-sections, scattering matrix, etc. are expressed through these coefficients (see, e.g., [61]).

One should realize that our selection of the scalar potentials U, V is equivalent to use of the corresponding vector wave functions in the field expansions. For instance, for the TE mode and the electric field, instead of Eqs. (6) and (8) we could write

$$\mathbf{E}_1^{(i)}(\mathbf{r}) = \mathbf{E}_{1,A}^{(i)}(\mathbf{r}) + \sum_{m=1}^{\infty} \sum_{l=m}^{\infty} (a_{1,lm}^{(i)} \mathbf{M}_{lm}^z(\mathbf{r}) + b_{1,lm}^{(i)} \mathbf{M}_{lm}^r(\mathbf{r})), \quad \mathbf{r} \in D_i, \quad (10)$$

where the vector wave functions are

$$\mathbf{M}_{lm}^z(\mathbf{r}) = \nabla \times (\mathbf{i}_z \psi_{lm}(\mathbf{r})), \quad \mathbf{M}_{lm}^r(\mathbf{r}) = \nabla \times (\mathbf{r} \psi_{lm}(\mathbf{r})). \quad (11)$$

Here $\psi_{lm}(\mathbf{r})$ is a solution to the scalar Helmholtz equation $\Delta\psi + k_i\psi = 0$.

It is easy to prove that the coefficients $a_{s,lm}^{(i)}$, $b_{s,lm}^{(i)}$ in Eqs. (8)–(10) are the same. Note that instead of our potentials U, V one can use two usual Debye potentials $V_{e,m}$ and correspondingly expand the fields in the functions \mathbf{M}_{lm}^z and $\mathbf{N}_{lm}^r = \nabla \times \mathbf{M}_{lm}^z$.

It should be noted that the axisymmetric task is actually scalar—one scalar potential ($p_s^{(i)}$ or $q_s^{(i)}$) defines the fields $\mathbf{E}_{s,A}^{(i)}$, $\mathbf{H}_{s,A}^{(i)}$ for each i, s . Hence solution of this task is simple and very fast. Our large experience of dealing with the axisymmetric and nonaxisymmetric tasks indicates that their properties (convergence behaviour, accuracy, etc.) are very close. It makes the axisymmetric task very useful in extensive studies of applicability ranges of different approaches. Solution of this task also allows one quickly to derive proper values of such technical parameters as the number of knots in quadrature formula and of terms kept in the expansions necessary to reach given accuracy of results. A back side of our extracting the axisymmetric part of the fields is that generally we need to keep 1–2 additional terms in the field (potential) expansions to have as high same accuracy as that obtained without extracting. If necessary, one can skip this extraction simply by taking $m = 0$ in Eq. (10).

2.3. Linear systems to be solved

The systems of linear algebraic equations relative to the scattered field expansion coefficients are derived as follows. We write the boundary conditions (2) separately for the axisymmetric ($\mathbf{E}_A, \mathbf{H}_A$) and nonaxisymmetric ($\mathbf{E}_N, \mathbf{H}_N$) parts of the fields and replace these field parts with the corresponding scalar potentials, using Eqs. (5)–(7). The potential expansions (8)–(9) are substituted in the reformulated boundary conditions. The conditions for each boundary are then multiplied by functions $P_n^m(\cos \theta) \sin m\theta$ and integrated over the corresponding surface S_i . Completeness of the spherical functions allows one to get systems of linear algebraic equations relative to the expansion coefficients of the scattered field and all internal ones.

In the axisymmetric task we consider the first N terms in the potential expansions and multiply the conditions written for p, q by N different spherical harmonics with $m = 1$. In the nonaxisymmetric task $N^2/2$ terms are kept in the U, V expansions and multiplication is made for $N - m + 1$ spherical harmonics with $m = 1, 2, \dots, N$.

For an axisymmetric scatterer, one can solve the systems arising for different m independently, and hereafter we skip the index m . So, for each m one gets finite systems which look in the matrix form as follows:

$$\begin{pmatrix} A^{(i)} & B^{(i)} \\ C^{(i)} & D^{(i)} \end{pmatrix} \begin{pmatrix} \mathbf{x}^{(i)} \\ \mathbf{y}^{(i)} \end{pmatrix} = \begin{pmatrix} E^{(i+1)} & F^{(i+1)} \\ G^{(i+1)} & H^{(i+1)} \end{pmatrix} \begin{pmatrix} \mathbf{x}^{(i+1)} \\ \mathbf{y}^{(i+1)} \end{pmatrix}, \quad i = 1, 2, \dots, \mathcal{L}. \quad (12)$$

For each m the vectors $\mathbf{x}^{(i)}$ and $\mathbf{y}^{(i)}$ contain the expansion coefficients $(\{a_{1,lm}^{(i)}\}_{l=m}^N, \{b_{1,lm}^{(i)}\}_{l=m}^N)$ and $(\{a_{2,lm}^{(i)}\}_{l=m}^N, \{b_{2,lm}^{(i)}\}_{l=m}^N)$, respectively. The elements of matrices $A^{(i)}, B^{(i)}, C^{(i)}, D^{(i)}$ are integrals of products of the Bessel or first kind Hankel functions and the associated Legendre functions (and their first derivatives) over the surface S_i , for instance

$$A_{m,nl}^{(i)} = \int_0^\pi j_l(k_i r_i(\theta)) P_l^m(\cos \theta) P_n^m(\cos \theta) \sin \theta d\theta, \quad (13)$$

where $r = r_i(\theta)$ is the surface equation of S_i . Expressions for other matrix elements are presented in [62]. Note that in the innermost layer $E_2^{\mathcal{L}+1} = 0$, i.e., $\mathbf{y}^{(\mathcal{L}+1)} = 0$ and one has

$$\begin{pmatrix} A^{(\mathcal{L})} & B^{(\mathcal{L})} \\ C^{(\mathcal{L})} & D^{(\mathcal{L})} \end{pmatrix} \begin{pmatrix} \mathbf{x}^{(\mathcal{L})} \\ \mathbf{y}^{(\mathcal{L})} \end{pmatrix} = \begin{pmatrix} E^{(\mathcal{L}+1)} \\ G^{(\mathcal{L}+1)} \end{pmatrix} \mathbf{x}^{(\mathcal{L}+1)}. \quad (14)$$

It should be pointed out that there are two alternative approaches to Eqs. (12)—one either composes one large system (see, e.g., [21,31,34] and most works on core-mantle particles) or avoids this by using recursive [25,26,33] or iterative [20,22,30,50] relations.

2.3.1. Single system approach

It is easy to bring the known vector $\mathbf{x}^{(1)}$ into the right-hand side of system (12) for $i = 1$ and to join partly related other systems for $i = 2, 3, \dots, \mathcal{L}$. This gives the following system relative to the unknown coefficients of expansions of the scattered and internal fields:

$$\begin{pmatrix} -B^{(1)} & E^{(2)} & F^{(2)} & 0 & \dots & 0 \\ -D^{(1)} & G^{(2)} & H^{(2)} & 0 & \dots & 0 \\ 0 & -A^{(2)} & -B^{(2)} & E^{(3)} & \dots & 0 \\ 0 & -C^{(2)} & -D^{(2)} & G^{(3)} & \dots & 0 \\ \dots & \dots & \dots & \dots & \dots & \dots \\ 0 & 0 & 0 & 0 & \dots & E^{(\mathcal{L}+1)} \\ 0 & 0 & 0 & 0 & \dots & G^{(\mathcal{L}+1)} \end{pmatrix} \begin{pmatrix} \mathbf{y}^{(1)} \\ \mathbf{x}^{(2)} \\ \mathbf{y}^{(2)} \\ \mathbf{x}^{(3)} \\ \vdots \\ \mathbf{y}^{(\mathcal{L})} \\ \mathbf{x}^{(\mathcal{L}+1)} \end{pmatrix} = \begin{pmatrix} A^{(1)} \\ C^{(1)} \\ 0 \\ 0 \\ \vdots \\ 0 \\ 0 \end{pmatrix} \mathbf{x}^{(1)}. \quad (15)$$

The dimension of this system is $2N\mathcal{L}$ in the axisymmetric task and $4(N+1-m)\mathcal{L}$ for $m = 1, 2, \dots, M$ in the nonaxisymmetric one. Usually, the number of azimuthal terms to be considered (M) can be essentially smaller than the number of radial ones (N).

An advantage of this approach is flexibility in choosing N as its different values can be selected in layers. This may be useful for scatterers with the layer surfaces of different types as convergence of methods mainly depends on surfaces' shape. However, the approach meets an obvious problem for particles with a large number of layers as the system size and computational time quickly grow with an increase of \mathcal{L} . This problem is solved by use of sparse matrix inversion algorithms [34].

2.3.2. Iteration/recursion approach

This approach to system (12) can be presented in different ways. For example, we introduce matrices P_1, P_2 so that

$$\begin{pmatrix} A^{(1)} & B^{(1)} \\ C^{(1)} & D^{(1)} \end{pmatrix} \begin{pmatrix} \mathbf{x}^{(1)} \\ \mathbf{y}^{(1)} \end{pmatrix} = \begin{pmatrix} P_1 \\ P_2 \end{pmatrix} \mathbf{x}^{(\mathcal{L}+1)}. \quad (16)$$

The matrices P_1, P_2 are easily derived by considering Eq. (12) with the inverted left-hand side matrix consequently for $i = \mathcal{L}, \mathcal{L} - 1, \dots, 2$ and in its normal form for $i = 1$. This gives

$$\begin{pmatrix} P_1 \\ P_2 \end{pmatrix} = \begin{pmatrix} E^{(2)} & F^{(2)} \\ G^{(2)} & H^{(2)} \end{pmatrix} \left[\prod_{i=2}^{\mathcal{L}-1} \begin{pmatrix} A^{(i)} & B^{(i)} \\ C^{(i)} & D^{(i)} \end{pmatrix}^{-1} \begin{pmatrix} E^{(i+1)} & F^{(i+1)} \\ G^{(i+1)} & H^{(i+1)} \end{pmatrix} \right] \begin{pmatrix} A^{(\mathcal{L})} & B^{(\mathcal{L})} \\ C^{(\mathcal{L})} & D^{(\mathcal{L})} \end{pmatrix}^{-1} \begin{pmatrix} E^{(\mathcal{L}+1)} \\ G^{(\mathcal{L}+1)} \end{pmatrix}. \quad (17)$$

We solve the system that is obtained from Eq. (16)

$$\begin{pmatrix} -B^{(1)} & P_1 \\ -D^{(1)} & P_2 \end{pmatrix} \begin{pmatrix} \mathbf{y}^{(1)} \\ \mathbf{x}^{(\mathcal{L}+1)} \end{pmatrix} = \begin{pmatrix} A^{(1)} \\ C^{(1)} \end{pmatrix} \mathbf{x}^{(1)}. \quad (18)$$

Thus, here we make $\mathcal{L} - 1$ inversions of $2N \times 2N$ matrices in the axisymmetric part and $4(N+1-m) \times 4(N+1-m)$ matrices for each m to be considered in the nonaxisymmetric one. So, the algorithm is more robust to an increase of the number of layers than the single matrix scheme presented above.

Note that one can rewrite Eq. (17) as follows:

$$\begin{pmatrix} P_1 \\ P_2 \end{pmatrix} = \left[\prod_{i=2}^{\mathcal{L}} \begin{pmatrix} E^{(i)} & F^{(i)} \\ G^{(i)} & H^{(i)} \end{pmatrix} \begin{pmatrix} A^{(i)} & B^{(i)} \\ C^{(i)} & D^{(i)} \end{pmatrix}^{-1} \right] \begin{pmatrix} E^{(\mathcal{L}+1)} \\ G^{(\mathcal{L}+1)} \end{pmatrix}. \quad (19)$$

This rather iterative relation allows one easily to formulate a recursive relation for the matrices P_1, P_2

$$\begin{pmatrix} P_1(\mathcal{L}) \\ P_2(\mathcal{L}) \end{pmatrix} = \begin{pmatrix} E^{(2)} & F^{(2)} \\ G^{(2)} & H^{(2)} \end{pmatrix} \begin{pmatrix} A^{(2)} & B^{(2)} \\ C^{(2)} & D^{(2)} \end{pmatrix}^{-1} \begin{pmatrix} P_1(\mathcal{L}-1) \\ P_2(\mathcal{L}-1) \end{pmatrix}, \quad (20)$$

where $P_s(L)$ means the matrix P_s for a particle with L layers ($s = 1, 2$) and the innermost layer of an \mathcal{L} -layered particle is characterized by the matrices $A^{(2)}, B^{(2)}, \dots, H^{(2)}$.

Instead of solution of a linear system one often calculates a T -matrix that relates the unknown and known field expansion coefficients in the form $\mathbf{y}^{(1)} = T\mathbf{x}^{(1)}$. In our case the T -matrix is equal to

$$T = (A^{(1)} - P_1 P_2^{-1} C^{(1)})^{-1} (B^{(1)} - P_1 P_2^{-1} D^{(1)}). \quad (21)$$

Note that in an earlier paper [62] we used other auxiliary matrices Q_1, Q_2 defined by relation

$$\begin{pmatrix} \mathbf{x}^{(1)} \\ \mathbf{y}^{(1)} \end{pmatrix} = \begin{pmatrix} Q_1 \\ Q_2 \end{pmatrix} \mathbf{x}^{(\mathcal{L}+1)}. \quad (22)$$

This gave a more simple expression for the T -matrix

$$T = Q_2 Q_1^{-1}. \quad (23)$$

However, our use of Q_1, Q_2 and Eq. (22) instead of P_1, P_2 and Eq. (18) surprisingly led to several order lower accuracy that could be reached.

It should be noted that Peterson and Ström [25] suggested a simple recursive relation for T -matrices of layered scatterers. It may be written as

$$T(\mathcal{L}) = (Q_{11} - Q_{13} T(\mathcal{L}-1))(Q_{31} - Q_{33} T(\mathcal{L}-1))^{-1}, \quad (24)$$

where $T(\mathcal{L})$ is the T -matrix of an \mathcal{L} -layered particle and Q_{ij} are some matrices described, e.g., in [26]. Obviously, Eq. (24) is applicable to the T -matrices arisen in our axisymmetric and nonaxisymmetric tasks with

$$T(1) = G^{(\mathcal{L}+1)} (E^{(\mathcal{L}+1)})^{-1}. \quad (25)$$

However, our paper [50] demonstrates that an iterative scheme for the T -matrices being generally equivalent to the recursive relation (24) should be more computationally efficient

$$\begin{pmatrix} Q_1(\mathcal{L}) \\ Q_2(\mathcal{L}) \end{pmatrix} = \prod_{i=2}^{\mathcal{L}} \begin{pmatrix} Q_{31}^{(i)} & -Q_{33}^{(i)} \\ Q_{11}^{(i)} & -Q_{13}^{(i)} \end{pmatrix} \begin{pmatrix} Q_1(1) \\ Q_2(1) \end{pmatrix}. \quad (26)$$

When the EBCM method is applied, elements of the matrices $Q_{jk}^{(i)}$ and $Q_j(1)$ are some surface integrals and use of the iterative scheme (26) allows one to avoid \mathcal{L} inversions of the matrix $\tilde{Q}_1 = (Q_{31} - Q_{33} T)$ made in the recursion relation (24). In the SVM method an extra inversion of \tilde{Q}_1 to get T -matrix at each step in the recursion scheme is less essential as a matrix including A, B, C, D is anyway inverted for each i to get the matrix with $Q_{jk}^{(i)}$.

So, we see that the iterative and recursive schemes are tightly related and present an alternative to the single matrix scheme described above. Use of the matrices P_1, P_2 or Q_1, Q_2 looks to be preferable to that of the T -matrices and then there is practically no difference between iterative and recursive schemes.

3. Numerical results and discussion

We have implemented the suggested SVM approach to layered nonspherical scatterers as a Fortran 77 code. Both alternative schemes of solution of the equation system were included. All computations were performed with an Intel 1.8 Hz processor.

3.1. Convergence, accuracy and computational time

These three related aspects of our code in the case of layered spheroids are reflected in Fig. 2, where we consider how a measure of relative accuracy of results—relative difference of the extinction and scattering cross-sections for nonabsorbing particles

$$\delta = \frac{|C_{\text{ext}} - C_{\text{sca}}|}{C_{\text{ext}} + C_{\text{sca}}} \quad (27)$$

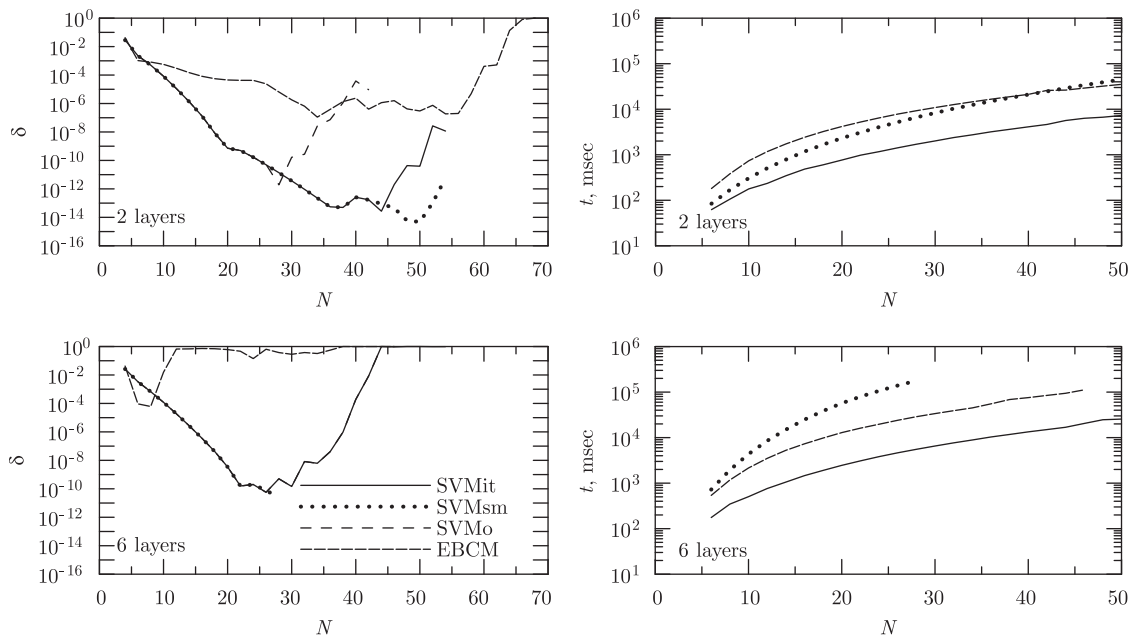


Fig. 2. Dependence of an error measure δ (left panels) and computational time t (right panels) on the number of terms N kept in the field expansions for 2 and 6-layered prolate spheroids. The aspect ratio of the layer surfaces is the same ($a_i/b_i = 1.5$), the size parameters $x_{v,1} = 3$, $x_{v,i} = x_{v,i-1} - 0.25$, refractive index outside the particle $m_1 = 1$ and in even and odd layers $m_i = 1.33$ and 1.7 , respectively, the incident wave propagation angle $\alpha = 45^\circ$. Results were obtained with our SVM code for the single matrix (SVMsm) and iterative (SVMit) schemes and with the EBCM code from [50].

and computational time t depend on the number of terms kept in the field (potential) expansions N for prolate spheroids with cyclically repeating layers of several materials. The behaviour of accuracy reflected in the dependence $\delta(N)$ is typical of the SVM, EBCM and PMM methods—when N grows, accuracy first increases but after some value of N rapidly decreases [59]. Similar figures were obtained for another accuracy measure—relative difference in a cross-section obtained when N and $N - 1$ terms are considered

$$\delta_N = \frac{|C_N - C_{N-1}|}{C_{N-1}}. \quad (28)$$

The dependence of computational time on N may be approximated as $t \sim N^\alpha$ with $\alpha = 2.5 - 3$, which is also typical of the methods. The data given for the EBCM are discussed in the next subsection.

Comparing two alternative schemes, one can conclude from Fig. 2 that use of a big system allows one to reach better accuracy than application of an iterative/recursive relation. The convergence speed (here the slope of $\delta(N)$) is nearly the same, but the former approach is 2–100 times slower than the latter one and this difference grows with N and in particular with the number of layers \mathcal{L} . Note that standard Gauss–Jordan matrix elimination subroutines used to crash when the number of equations exceeds about 500–1000 (as seen in Fig. 2) and further one should apply sparse matrix inversion procedures.

The upper left panel also demonstrates results from the paper [62] where we used Eqs. (22) instead of Eqs. (18). As a result, maximum accuracy reached was lower by a factor of 100, though with an increase of \mathcal{L} this difference decreased.

One can also see that the convergence speed does not depend on the number of layers \mathcal{L} , while maximum accuracy reached does. It is still very high (about 10^{-10}) for a spheroid with six layers. So, even for a scatterer with 100 layers one should get several correct digits in results. Required computational time nearly linearly grows with the number of layers when the iteration scheme is applied.

3.2. Comparison with other methods

We have compared our SVM code for layered scatterers with available codes based on other methods, namely the EBCM, GMT and DDA. Fig. 3 shows the phase function computed for 2 to 100-layered spheroids by our code, a GMT code from [34] and (for $\mathcal{L} \leq 10$) the standard DDA code [35].

The GMT method described in [34] is often called the null field method with discrete sources (and sometimes a TMM). The book [34] well explains the method where the fields are expanded in terms of spherical functions at different points

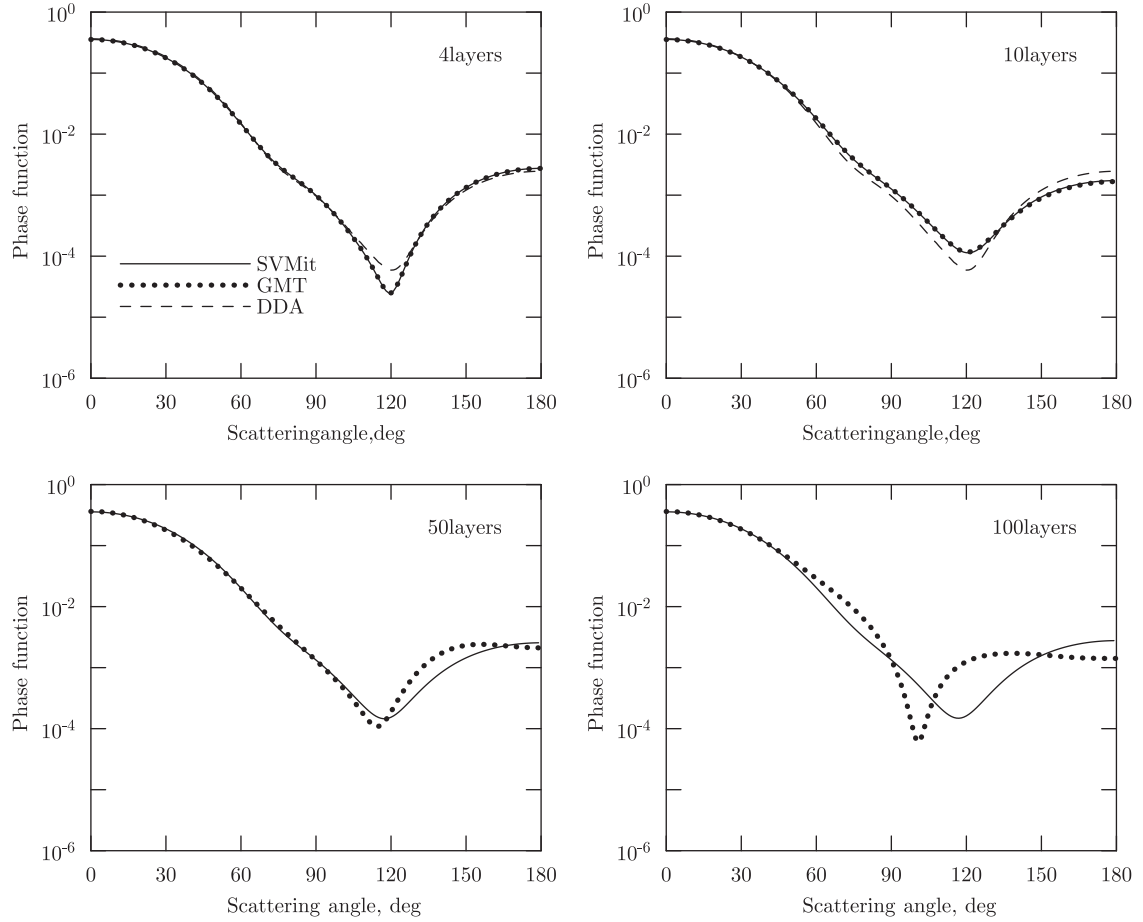


Fig. 3. Phase function computed by the SVM, GMT and DDA methods for a multilayered prolate spheroid. Equivolume layers consist of vacuum ($m = 1$) and ice ($m = 1.33$) with their volume fractions being equal to 0.33 and 0.67, respectively. The aspect ratio of the layer surfaces is the same ($a_i/b_i = 1.5$), the particle size parameter $x_V = 3$, the axial incidence ($\alpha = 0^\circ$).

Table 1
Normalized cross-sections obtained with the SVM and GMT codes.

\mathcal{L}	SVM			GMT		
	N	Q_{sca}	Q_{ext}	N	Q_{sca}	Q_{ext}
2	38	0.832175034371	0.832175034371	10	0.8322	0.8323
6	34	0.86357148727	0.86357148726	8	0.8636	0.8630
8	30	0.87266563639	0.87266563640	10	0.8722	0.8723
10	30	0.87911779316	0.87911779317	8	0.878	0.876
50	20	0.9065868	0.9065863	8	0.88	0.89
100	20	0.911002	0.911004	8	0.9	0.8

(sources) $\{\mathbf{r}_n\}_{n=1}^N$, which can be presented in our notation like the following (cf. Eq. (10)):

$$\mathbf{E}_1^{(i)}(\mathbf{r}) = \sum_{m=0}^{M_{rank}} \sum_{n=1}^{N_{rank}} (a_{nm}^{(i)} \mathbf{M}_{m,m+l}^r(\mathbf{r} - \mathbf{r}_n^{(i)}) + b_{nm}^{(i)} \mathbf{N}_{m,m+l}^r(\mathbf{r} - \mathbf{r}_n^{(i)})), \quad (29)$$

where $l = 1$ for $m = 0$ and $l = 0$ otherwise. The GMT code was configured to choose sources automatically, the number of integration points was $N_{int} = 1000$, the number of expansions N_{rank} was varying from 4 to 40 but kept the same for all layers, the number of azimuthal expansions M_{rank} was determined by the code automatically. The figure demonstrates that the results obtained with the GMT and our SVM codes match very well for particles with up to 10 layers. Essential difference at large scattering angles can be observed only for a very large number of layers. A deeper insight in accuracy of the results is provided by Table 1 where we give normalized extinction and scattering cross-sections for the spheroids

considered in Fig. 3. Computational time required by the GMT and our SVM codes to obtain the data in the table was comparable. This may be related only with a large number of integration points used to be taken in the GMT code as generally this method should be faster than the SVM. Table 1 indicates a good match of the SVM results with the law of conservation of energy (Q_{ext} is equal to Q_{sca} for dielectric particles). This fact shows that the proposed SVM method is very robust to an increase of the layer number and should provide reliable results even for particles with more than a hundred of layers.

The DDA code applied is a very popular CDM tool employed to solve the light scattering problem for nonspherical inhomogeneous particles. We added a simple subroutine modelling dipole locations for a multilayered particle (target) and used the basic code described in [35]. The total number of dipoles was $N_{\text{dip}} = 1.5 \times 10^6$, but similar results were obtained also for $N_{\text{dip}} = 10^5$. There is a problem of the DDA method when applied to scatterers with a large (over about 10) number of layers—it becomes hardly possible to keep the correct volume fractions of materials involved as the layers become too narrow for appropriate distribution of dipoles even when N_{dip} exceeds millions. Hence in Fig. 3 we present only data obtained for 4 and 10-layered particles. One can well see how small difference between the DDA and other methods for $\mathcal{L} = 4$ becomes essential for $\mathcal{L} = 10$. Nevertheless, the DDA being also a rather slow method is still very useful in treatment of complex scatterers with a few layers.

The EBCM code used was described in [50]. It includes an iterative scheme based on Eq. (22) that could be improved as discussed above. Further improvement of performance of the code can be expected after use of the approach utilized in the well-known EBCM/TMM code of Mishchenko [1]. However, Fig. 2 has clearly demonstrated that the EBCM method is not quite suitable for treatment of layered scatterers. The reason may be in the fact observed for homogeneous particles for which the applicability range of the EBCM (in contrast to the PMM and SVM) is strictly limited in space of particle shape parameters (see discussion in [59]). When more shapes (of layers) are involved, this range quickly decreases. An illustration is Fig. 4 for core-mantle spheroids. It is well seen from the figure that the EBCM provides acceptable accuracy only for the aspect ratio $a_1/b_1 < \sqrt{2}$ (while the SVM works well beyond this limit). Note that for homogeneous spheroids the EBCM gives accurate cross-sections for $a/b > 4-10$. When more layers are considered, convergence of the EBCM becomes worse (see Fig. 2) and one can hardly obtain reliable results for the number of layers larger than 5.

3.3. Illustrative examples

To illustrate capacity of the method and code suggested, we present some more numerical results obtained for porous particles. Figs. 5 and 6 show normalized scattering cross-section and phase function, respectively, for spheroids with

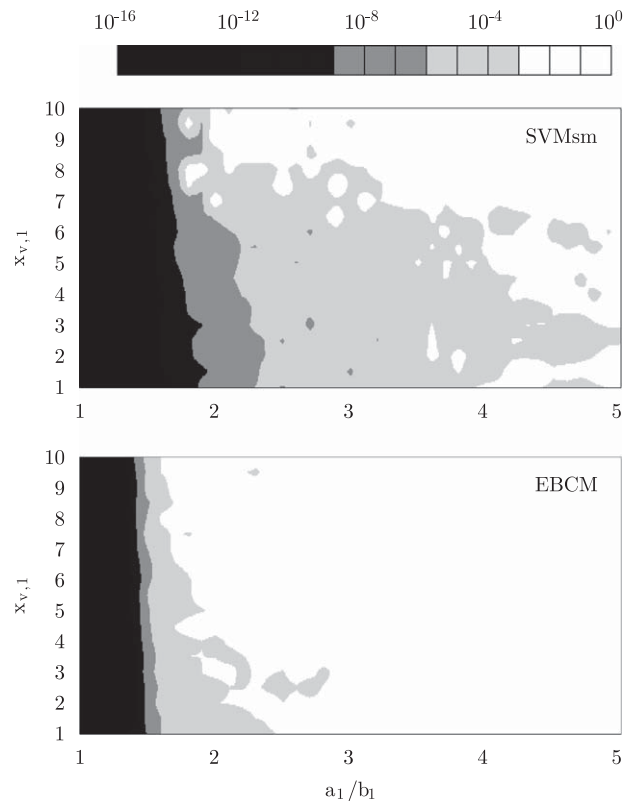


Fig. 4. Accuracy of cross-sections of core-mantle spheroids achieved by the SVM and EBCM methods in dependence on the particle aspect ratio a_1/b_1 and the size parameter $x_{v,1}$. Other parameters are as in Fig. 2.

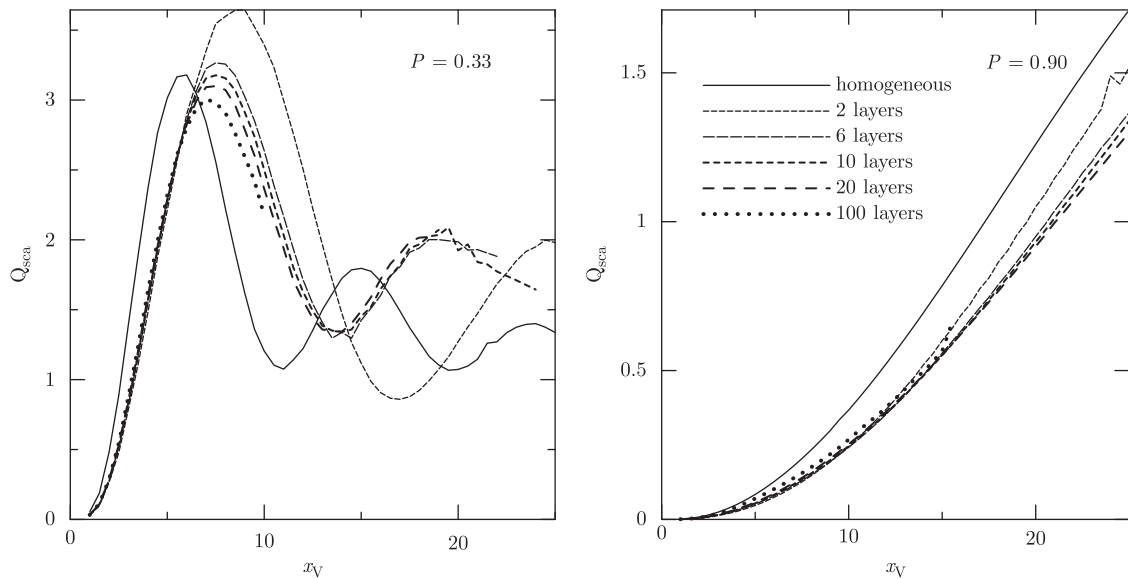


Fig. 5. Normalized scattering cross-section Q_{sca} in dependence on the size parameter x_V for 2, 6, 10, 20, and 100-layered prolate spheroids. Materials of equivolume layers are vacuum ($m = 1$) and dirty ice ($m = 1.33 + i0.01$). The volume fraction of vacuum (porosity) is 0.33 (left panel) and 0.9 (right panel). The aspect ratio of all layers is the same $a_i/b_i = 1.5$, the axial incidence ($\alpha = 0^\circ$). For homogeneous spheres, refractive index was obtained using the Maxwell–Garnett rule.

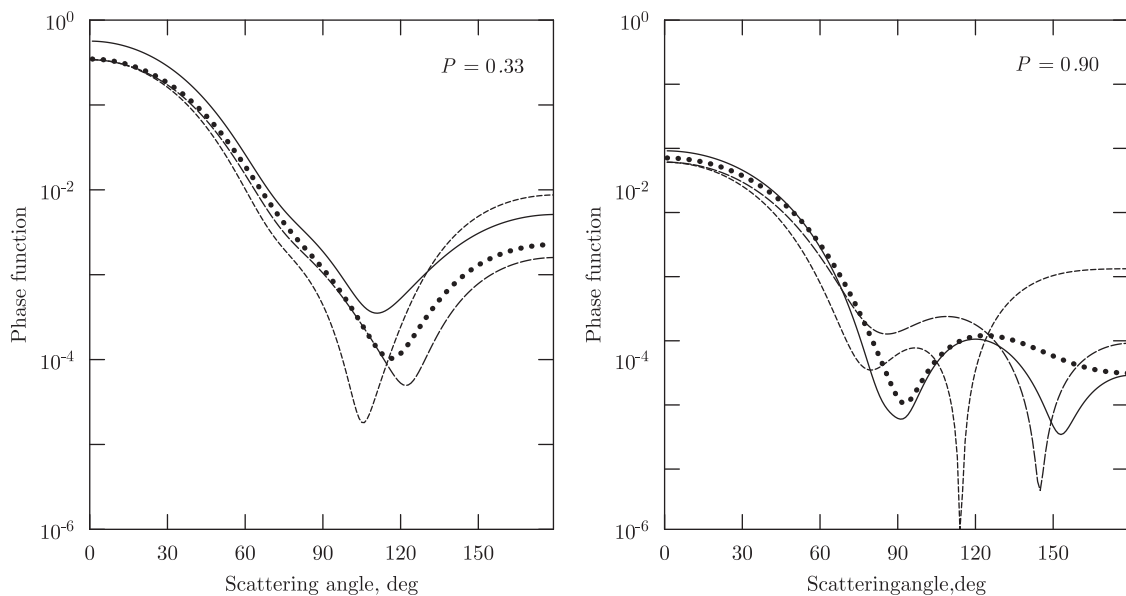


Fig. 6. Phase function for 2, 6, 10, 20 and 100-layered spheroids. The outermost layer size parameter $x_{V,1} = 3$, other parameters are as in Fig. 5.

cyclically repeating layers of ice and vacuum. The number of layers \mathcal{L} changes from 2 to 100 for two values of particle porosity (the volume fraction of vacuum) $P = 0.33$ and 0.9. Note that the (integral) cross-section for $P = 0.9$ and the phase function (differential cross-section) for $P = 0.33$ rather weakly depend on \mathcal{L} when $\mathcal{L} > 4$. In contrast, this cross-section for $P = 0.33$ and the phase function for $P = 0.9$ essentially change with an increase of \mathcal{L} even when $\mathcal{L} \sim 100$.

We believe that there should be some limit values of the cross-section and the phase function as the number of layers tends to infinity. It took place for layered spheres considered in [63], where its author needed, however, about several thousands of layers to approach this limit. The behaviour of Figs. 5–6 confirms this conclusion for spheroids.

The results presented in this section make more understandable the following Table 2 where we very roughly estimate properties of the methods mentioned in Section 1 when they are applied to layered scatterers. The table shows the type of scatterers to which the given method is applicable, a maximum reachable size parameter $x_V = 2\pi r_V/\lambda$, where r_V is the radius of a sphere which volume is equal to that of a nonspherical particle, a maximum aspect ratio a/b when the method is

Table 2

Methods applied to layered nonspherical scatterers.

Method ^a	Particle type	x_v	a/b	\mathcal{L}	Accuracy	Speed
EMT	Any ^b	Medium to large ^b	Medium to large ^b	Any	Low	High
RA	Confocal ellipsoids ^c	Small	Medium to large ^d	Any	Medium to low	High
GMT	Any	Medium	Medium to large	Large	Medium to high	Medium
SVM ^e	Axisymmetric	Medium	Medium	Large	High	Medium
EBCM	Axisymmetric ^f	Medium ^g	Medium ^g	Small	High	Medium
SVMsph ^h	Confocal spheroids ⁱ	Large	Large	Large	High	Medium
CDM	Any	Medium	Large	Medium ^j	Medium	Low
FDTD ^k	Any	Medium(?)	Large(?)	Medium(?)	Medium(?)	Low

^a See the names of the methods in Section 1.^b Depends on the method used for homogeneous particles with an effective refractive index.^c Properties of an extension to nonconfocal ellipsoids in [46] are not clear.^d Large for so called quasistatic approximation [46].^e The method developed in this work.^f For nonaxisymmetric scatterers the speed becomes rather low.^g Medium to large when extended precision is used.^h SVM with a spheroidal basis.ⁱ Properties of an extension to nonconfocal spheroids in [24] are not clear.^j When dipoles form a cubic lattice.^k Properties of the FDTD method when applied to layered scatterers are not quite clear.

applied to spheroidal scatterers, a possible number of layers \mathcal{L} , accuracy of results and speed of the method relative to others. The table is *not a verdict* for the methods, but just a background to better realize the place of the suggested approach (labelled by SVM in the table) among others. We see that our method can be useful when one needs rather efficiently to treat simple shape nonspherical scatterers with a (very) large number of layers if these particles are more complex than spheroids with the confocal layer boundaries. Note that such spheroids form a very special set of particles as any layer shape is strictly determined by its volume and the particle aspect ratio. Our method can also be applied when one requires (very) high accuracy of results for layered scatterers of a simple shape. It may be in particular useful as a testing tool for other codes.

4. Conclusions

We have developed a special version of the SVM method for axisymmetric multilayered scatterers. Numerical tests show that our approach provides high accuracy results for simple shape particles with up to 100 layers.

A consideration of two general computational schemes used for layered scatterers has been performed. We find that the single system scheme allows one usually to reach more accurate results than the iterative or recursive scheme. However, the former requires an order of magnitude longer computational time than the latter and is hardly applicable to scatterers with 10 and more layers without use of sparse matrix inversion algorithms.

Comparison of the developed SVM code with available codes based on other (EBCM, GMT, DDA) methods applicable to layered particles allows one to see the field of applicability of our code. It should be most useful for treatment of layered particles being more complex than spheroids with strictly confocal layer boundaries and having a rather large number of layers or any number of layers if high accuracy of results is required. Note that solution of these tasks is hardly possible by other light scattering methods.

Acknowledgements

The authors are thankful to B. Draine and Th. Wriedt for providing the DDA and GMT codes, respectively, and M. Prokopjeva for performing calculations with the DDA code.

The work was partly supported by the Grants RFFI 07-02-00831, NTP 2.1.1/665 and NSH 1318.2008.2.

References

- [1] Mishchenko MI, Hovenier JW, Travis LD. Light scattering by nonspherical particles. San Diego: Academic Press; 2000.
- [2] Kahnert FM. Numerical methods in electromagnetic scattering theory. JQSRT 2003;79–80:775–824.
- [3] Mie G. Beiträge zur Optik Trüber Medien, speziell kolloidaler Metallösungen. Ann Phys 1908;25:377–445.
- [4] Fuller KA, Mackowski DW. Electromagnetic scattering by compounded spherical particles. In: Mishchenko MI, Hovenier JW, Travis LD, editors. Light scattering by nonspherical particles. San Diego: Academic Press; 2000. p. 225–72.
- [5] Aden AL, Kerker M. Scattering of electromagnetic waves from two concentric spheres. J Appl Phys 1951;22:1242–6.

- [6] Gonzales F, Moreno F. Introduction to light scattering from microstructures. In: Moreno F, Gonzales F, editors. Light scattering from microstructures. Lectures notes in physics, vol. 534. Berlin: Springer; 2000. p. 1–19.
- [7] Babenko VA, Astafyeva LG, Kuzmin VN. Electromagnetic scattering by disperse media. London: Springer-Praxis; 2003.
- [8] Gurwicz I, Shiloah N, Kleiman M. Calculations of the Mie scattering coefficients for multilayered particles with large size parameters. *JQSRT* 2001;70:433–40.
- [9] Yang W. Improved recursive algorithm for light scattering by a multilayered sphere. *Appl Opt* 2003;42:1710–20.
- [10] Li R, Han X, Jiang H, Ren KF. Debye series for light scattering by a multilayered sphere. *Appl Opt* 2006;45:1260–70.
- [11] Li R, Han X, Shi L, Ren KF, Jiang H. Debye series for Gaussian beam scattering by a multilayered sphere. *Appl Opt* 2007;46:4804–12.
- [12] Kerker M, Matijevich E. Scattering of electromagnetic waves from concentric infinite cylinders. *J Opt Soc Am* 1961;51:506–8.
- [13] Shah GA. Scattering of plane electromagnetic waves by infinite concentric circular cylinders at oblique incidence. *Mon Not R Astron Soc* 1970;148:93–102.
- [14] Yousif HA, Elsherbeni AZ. Electromagnetic scattering from an eccentric multilayered cylinder at oblique incidence. *J Electromagn Wave Appl* 1999;13:325–36.
- [15] Gurwicz I, Shiloah N, Kleiman M. The recursive algorithm for electromagnetic scattering by titled infinite circular multi-layered cylinder. *JQSRT* 1999;63:217–29.
- [16] Li R, Han X, Jiang H, Ren KF. Debye series of normally incident plane-wave scattering by an infinite multilayered cylinder. *Appl Opt* 2006;45:6255–62.
- [17] Onaka T. Light scattering by spheroidal grains. *Ann Tokyo Astron Obs* 1980;18:1–54.
- [18] Ciric IR, Cooray FR. Separation of variables for electromagnetic scattering by spheroidal particles. In: Mishchenko MI, Hovenier JW, Travis LD, editors. Light scattering by nonspherical particles. San Diego: Academic Press; 2000. p. 89–130.
- [19] Gurwicz I, Kleiman M, Shiloah N, Cohen A. Scattering of electromagnetic radiation by multilayered spheroidal particles: recursive procedure. *Appl Opt* 2000;39:470–7.
- [20] Gurwicz I, Kleiman M, Shiloah N, Oaknin D. Scattering by an arbitrary multi-layered spheroid: theory and numerical results. *JQSRT* 2003;79–80:649–60.
- [21] Barton JP. Internal, near-surface and scattered electromagnetic fields for a layered spheroid with arbitrary illumination. *Appl Opt* 2001;40:3598–607.
- [22] Farafonov VG. New recursive solution of the problem of scattering of electromagnetic radiation by multilayered spheroidal particles. *Opt Spectra* 2001;90:743–52.
- [23] Li LW, Kang XK, Leong MS. Spheroidal wave functions in electromagnetic theory. New York: Wiley; 2002.
- [24] Han Y, Zhang H, Sun X. Scattering of shaped beam by an arbitrarily oriented spheroid having layers with non-confocal boundaries. *Appl Phys B* 2006;84:485–92.
- [25] Peterson B, Ström S. *T*-matrix formulation of electromagnetic scattering multilayered scatterers. *Phys Rev D* 1974;10:2670–84.
- [26] Wang DS, Barber PW. Scattering by inhomogeneous nonspherical objects. *Appl Opt* 1979;18:1190–7.
- [27] Mishchenko MI, Videen G, Babenko VA, Khlebtsov NG, Wriedt T. *T*-matrix theory of electromagnetic scattering by particles and its applications: a comprehensive reference database. *JQSRT* 2004;88:357–406.
- [28] Mishchenko MI, Videen G, Babenko VA, Khlebtsov NG, Wriedt T. Comprehensive *T*-matrix reference database: a 2004–2006 update. *JQSRT* 2007;106:304–24.
- [29] Mishchenko MI, Videen G, Babenko VA, Khlebtsov NG, Wriedt T, Zakharova NT. Comprehensive *T*-matrix reference database: a 2006–2007 update. *JQSRT* 2008;109:1447–60.
- [30] Petrov D, Shkuratov Y, Zubko E, Videen G. *Sh*-matrices method as applied to scattering by particles with layered structure. *JQSRT* 2007;106:437–54.
- [31] Kyurkchan AG, Demin DB, Orlova NI. Solution based on the pattern equation method for scattering of electromagnetic waves by objects coated with dielectric materials. *JQSRT* 2007;106:192–202.
- [32] Al-Rizzo HM, Tranquilla JM. Electromagnetic scattering from dielectrically coated axisymmetric objects using the generalized point-matching technique II. Numerical results and comparison. *J Comput Phys* 1995;119:356–73.
- [33] Doicu A, Wriedt T. Null-field method with discrete sources to electromagnetic scattering from layered scatterers. *Comput Phys Commun* 2001;138:136–42.
- [34] Doicu A, Wriedt T, Eremin Y. Light scattering by systems of particles. Berlin: Springer; 2006.
- [35] Draine BT, Flatau PJ. User guide for the discrete dipole approximation code DDSCAT 6.1. arXiv preprint: astro-ph/0409262; 2004.
- [36] Gordon HR, Du T. Light scattering by nonspherical particles: application to coccoliths detached from *Emiliania huxleyi*. *Limnol Oceanogr* 2001;46:1438–54.
- [37] Somasiri NP, Chen X, Robertson ID, Rezazadeh AA. Comparison of numerical techniques for full wave analysis of multi-layered microstrip antenna. *Int J Infrared Millim Waves* 2002;23:1777–85.
- [38] Kim J, Rahmat-Samii Y. Simulations, design and characterization of implanted antennas inside a human body. *IEEE Trans Microwave Theory Tech* 2004;52:1934–43.
- [39] Karlowski A. Improving accuracy of FDTD simulations in layered biological tissues. *IEEE Microwave Wireless Components Lett* 2004;14:151–2.
- [40] Winton SC, Kosmas P, Rappaport CM. FDTD simulations of TE and TM plane waves at nonzero incidence in arbitrary layered media. *IEEE Trans Antennas Propag* 2006;53:1721–8.
- [41] Choi MK. Numerical calculation of light scattering from a layered sphere by boundary-element method. *J Opt Soc Am* 2001;18:577–83.
- [42] Rysakov W, Ston M. The light scattering by core-mantle sphere. *JQSRT* 2001;69:121–9.
- [43] Seydou F, Duraiswami R, Gumerov NA, Seppänen T. TM electromagnetic scattering from multilayered dielectric bodies—numerical solution. *ACES J* 2004;19:100–7.
- [44] Medgyesi-Mitschang LN, Eftimiou C. Scattering from axisymmetric obstacles embedded in axisymmetric dielectrics: the method of moments. *Appl Phys* 1979;19:275–85.
- [45] Posselt B, Farafonov VG, Il'in VB, Prokopjeva MS. Light scattering by multilayered ellipsoidal particles in the quasistatic approximation. *Meas Sci Technol* 2002;13:256–62.
- [46] Sloat PMA, Fidgor CG. Elastic light scattering from nucleated blood cells: rapid numerical analysis. *Appl Opt* 1986;25:3559–65.
- [47] Kokhanovsky AA. Optics of light scattering media: problems and solutions. Berlin: Wiley-Praxis; 1999.
- [48] Bohren CF, Huffman DR. Absorption and scattering of light by small particles. New York: Wiley; 1983.
- [49] Farafonov VG, Il'in VB, Prokopjeva MS. Light scattering by multilayered nonspherical particles: a set of methods. *JQSRT* 2003;79–80:599–626.
- [50] Voshchinnikov VB, Il'in VB, Henning T. Modelling the optical properties of composite and porous interstellar grains. *Astron Astrophys* 2005;429:371–81.
- [51] Athanasiadis C. On the acoustic scattering amplitude for a multi-layered scatterer. *J Aust Math Soc Ser B* 1998;39:431–48.
- [52] Charalambopoulos A, Dassios G, Fotiadis DI, Massalas CV. Scattering of a point generated field by a multilayered spheroid. *Acta Mech* 2001;150:4107–19.
- [53] Gutman S. Identification of multilayered particles from scattering data by clustering method. *J Comput Phys* 2000;163:529–46.
- [54] Yan G, Zhao H. The far field operator for a multilayered scatterer. *Comput Math Appl* 2002;43:631–9.
- [55] Barton JP. Electromagnetic field calculations for an irregularly shaped near-spheroidal particle with arbitrary illumination. *J Opt Soc Am A* 2002;40:3598–607.
- [56] Farafonov VG, Vinokurov AA, Il'in VB. Comparison of the light-scattering methods using the spherical basis. *Opt Spektrosk* 2007;102:1006–16.
- [57] Farafonov VG. Diffraction of a plane electromagnetic wave by a dielectric spheroid. *Diff Equat (Sov)* 1983;19:1765–77.
- [58] Farafonov VG, Il'in VB. In: Kokhanovsky AA, editor. Light scattering reviews. Berlin: Springer-Praxis; 2006. p. 125–77.

- [60] Farafonov VG, Il'in VB. Single light scattering by simple model nonspherical heterogeneous particles. Berlin: Springer-Praxis; 2009, in preparation.
- [61] Voshchinnikov NV, Farafonov VG. Optical properties of spheroidal particles. *Astrophys Space Sci* 1993;204:19–86.
- [62] Farafonov VG, Vinokurov AA. Light scattering by multilayered axisymmetric particles: solution of the problem by the separation of variables method. *Opt Spektrosk* 2008;105:318–31.
- [63] Johnson BR. Exact theory of electromagnetic scattering by a heterogeneous multilayered sphere in the infinite-layer limit: effective-media approach. *J Opt Soc Am* 1999;16:845–52.